LWT - Food Science and Technology 115 (2019) 107884

Contents lists available at ScienceDirect

LWT - Food Science and Technology

journal homepage: www.elsevier.com/locate/lwt

Optimization of limonene microencapsulation based on native and fibril soy protein isolate by VIKOR method

Elham Ansarifar[a], Fakhri Shahidi[a,*], Mohebbat Mohebbi[a], Navid Ramezanian[b], Arash Koocheki[a], Amirhossein Mohamadian[c]

[a] Department of Food Science and Technology, Faculty of Agriculture, Ferdowsi University of Mashhad (FUM), Mashhad, Iran
[b] Department of Chemistry, Faculty of Science, Ferdowsi University of Mashhad (FUM), Mashhad, Iran
[c] Department of Food Science and Technology, Tarbiat modares University, Tehran, Iran

ARTICLE INFO

Keywords:
Fibril
Soy protein isolated
Emulsion system
Microencapsulation
VIKOR method

ABSTRACT

Fibril from food-grade materials is an important fundamental area of current researches in food systems. At first, in this study emulsifying properties of non-heated soy protein isolate (native SPI) and SPI fibril were compared. Then, the optimal concentration of SPI fibril was selected for microencapsulation of limonene by VIKOR method. The results indicated that SPI fibril interfacial tension oil/water (O/W) (5.88 mN/m) emulsion droplet size decreased and encapsulation efficiency (65.47%) was raised. The emulsifying activity index (EAI) (38.02 m^2/g) and emulsion stability index (ESI) (23.5 min) of the emulsion prepared with 1% (w/v) SPI fibril were significantly higher than (31.21 m^2/g and 15 min, respectively) of the native SPI. SEM images showed that the microcapsules obtained from the SPI fibril were smaller, more homogenous and smoother in their surfaces. The performance of the SPI fibril was better in forming and stabilizing the emulsion than the native SPI at the same concentration, based on the FTIR spectrum. VIKOR method was applied to obtain the best concentration of SPI fibril by ranking the scenarios, which its concentration of 0.5% (w/v) SPI fibril was chosen as the best. This study illustrated that SPI fibril can improve the emulsifying properties and microencapsulation efficiency of flavor and active cores.

1. Introduction

Protein fibrils with a length of about 1 μm and a diameter of 1–10 nm, are generated by heating globular protein at acidic pH and low ionic strength for several hours (Akkermans, van der Goot, Venema, van der Linden, & Boom, 2008). Currently, interest in fibrils as structural components in functional foods has led the research priorities to be considered as fibril formation (Chang et al., 2016; Isa, Jung, & Mezzenga, 2011; Jordens et al., 2014; Loveday, Wang, Rao, Anema, & Singh, 2012). The large aspect ratio of the fibrils to form a gel at lower protein concentrations, leads that protein fibrils have got potential applications as gelling and thickening agent, immobilization of enzymes and tissue engineering (Loveday et al., 2012). Also protein fibrils were shown to be surface active (Isa et al., 2011; Jordens et al., 2014) and were used to microencapsulate lipophilic ingredients (Serfert et al., 2014) and bioactive compounds (K. Humblet-Hua, Scheltens, Van Der Linden, & Sagis, 2011; Loveday et al., 2012). However, the emulsifying properties of fibrils has not been investigated largely. The fibrils may be improved emulsification properties compared to native protein because fibrils effectively prevent the occurrence of bridging flocculation in fibril-stabilized emulsions (Serfert et al., 2014). Soy protein isolates are widely used as ingredients in food products. So far, no studies are available with regards to examining the application of soy protein isolate fibrils for emulsification and microencapsulation of active component and flavor.

Since limonene is insoluble in water and easy to oxidative degradation, it is difficult to keep the lemon-like flavor especially in the areas such as water-rich phases and liquid-solid interfaces. Therefore, it is very important and necessary to utilize a delivery system to protect limonene from chemical degradation and improve its water-solubility. Recently, much attention has been paid to emulsion technology to solve the above problem (Wen, Yuan, Liang, & Vriesekoop, 2014).

There are many factors to selective optimum coating material concentration for microencapsulation process. The combination of criteria is important and can provide only one result as selection of best concentration. Therefore, we utilized the VIKOR method (Vlse Kriterijumska Optimizacija I Kompromisno Resenje in serbian, means Multicriteria Optimization and Compromise Solution), is commonly

* Corresponding author. Tel.: +989155161428; fax: +985138787430.
E-mail address: fshahidi@um.ac.ir (F. Shahidi).

https://doi.org/10.1016/j.lwt.2019.02.071
Received 19 July 2018; Received in revised form 18 December 2018; Accepted 23 February 2019
Available online 28 February 2019
0023-6438/

used in scientific research for optimization (Opricovic & Tzeng, 2004). It was originally developed to solve decision making problem with several conflicting and non-commensurable (different units) criteria (Opricovic & Tzeng, 2007). The compromise solution is a feasible solution, which is the closest to the ideal, and compromise means an agreement established by mutual concessions. However, this method offers more flexibility than other methods and will provide a compromise solution to conflicting data, but there is no article in the food science in the context.

Therefore, the objective of this work was to study the use of SPI fibril as a primary emulsifier for production of limonene-in-water (O/W) emulsion and microcapsulation of limonene by spray drying and its comparison to native SPI. This study applied the VIKOR method to assess the optimal concentration of SPI fibril.

2. Materials and methods

2.1. Materials

Food grade soy protein isolate (SPI) was obtained from Beh Pars Co., Iran (94% protein), (R)-(+)-limonene 97% was obtained from Sigma-Aldrich Co., Missouri, USA (CAS-no. 5989-27-5). All solutions were prepared with distilled and de-ionized water. All other chemicals were analytical grade, unless stated.

2.2. Methods

2.2.1. Production of soy protein isolate fibrils

SPI solution was prepared at a concentration of 6% w/v SPI in water and the pH was adjusted to 2 using 1 M HCl solution. The SPI solution was stirred 24 h at 4 °C. After that, the solution was centrifuged at 22600 × *g* for 30 min at 4 °C to remove un-dissolved materials. The fibrils were prepared by heating SPI solution at 80 °C for 24 h under continuous stirring. Then, the sample was quenched by cooling the samples immediately on ice, and freeze-dried (Martin Christ, 8891, Germany) under 0.9 mbar vacuum and temperature of −30 °C for 48 h (Akkermans et al., 2008).

2.2.2. Physicochemical characterization of SPI fibril

Fluorescence measurements with Thioflavin T (ThT): Measurements were carried out using the method based on that of Loveday et al. (Loveday et al., 2012). ThT binds to β-sheets present in the fibrils and thus the amount of fibrils can be measured (Akkermans et al., 2008). The assay solution (50 mM HCl, 100 Mm NaCl, 5–20 μM ThT, 20 μg mL^{-1} protein, pH 7.5) was excited at 450 nm with a slit width of 5 nm, and the emission was measured over a range that included the wavelength of 482 nm with width a slit width of 10 nm. Samples were taken every 1 h during 24 h incubation at 85 °C.

Transmission electron microscopy (TEM) and atomic force microscopy (AFM) of SPI-fibril:

SPI fibrils were also evaluated using Transmission electron microscopy (TEM, LEO 912 tab, Zeiss Germany) and atomic force microscopy (AFM, Ara research, model: Full plus, Iran). The sample preparation method was carried out as described in the literature (Akkermans et al., 2008).

2.2.3. Preparation of emulsion with native and fibril-SPI as emulsifier

For emulsification, an emulsion was prepared dispersing 1% w/v limonene in pH adjusted (pH = 3.5) deionized water containing 0.1, 0.3, 0.5, 1, 1.5 and 2% w/v SPI fibril or 1% w/v native SPI by laboratory rotor stator homogenizer (Ultra Turrax T-25, IKA Instruments, Germany) at a speed of 13500 rpm for 90 S the emulsion was further homogenized by sonication for 2 min using a 20 kHz ultrasonic processor (model VCX 750, Sonics & Materials, Inc., USA) operating at a nominal maximum power output of 750 W and equipped with a cylindrical titanium sonotrode (19 mm in diameter) immersed 1 cm below the surface of liquid. The temperature was kept constant at 20 °C throughout sonication by circulating cooling water through the jacket of chamber.

2.2.4. Physicochemical characterization of emulsion prepared with native and SPI fibril

Measurement of interfacial tension: The interfacial tension between D-limonene and water or SPI solution (0.1, 0.3, 0.5, 1, 1.5 and 2% w/v) was determined by Du Nouy ring method (Krüss K100 Tensiometer, Germany) at 20 °C, pH adjusted to 3.5. Droplets of limonene were dispensed from a J-shaped stainless steel needle into 45 mL of aqueous sample. Interfacial tension measurements were collected at 2 s intervals over a time span of 600 s. All measurements were carried out in triplicate.

Emulsion droplet size analysis and zeta potential: The droplet size distributions of the samples were determined by a laser diffraction particle sizer (Fritsch Analysette 22, Germany). The particle size was expressed as the mean volumetric size d_{43}, which is the mean diameter of a sphere with the same volume and is used to characterize a particle. Three measurements were performed on each sample. The zeta potential which is an indicator of surface charge was measured using a particle electrophoresis instrument (Zetasizer Nano ZS, Malvern Instrument, UK).

$$D32 = \sum nidi^3 / \sum nidi^2 \tag{1}$$

$$D43 = \sum nidi^4 / \sum nidi^3 \tag{2}$$

$$SSA = \frac{6\Phi}{D_{32}} (m^2 ml^{-1} emulsion) \tag{3}$$

Where n_i is the number of droplets of diameter d_i, Φ is the oil volume fraction of emulsion. To determine the distribution width of droplet size, an index known as span was calculated by the following Eq. (4):

$$span = \frac{[d(v.\ 90) - d(v.\ 10)]}{d(v.\ 50)} \tag{4}$$

where, d (v, 10), d (v, 50), and d (v, 90) are diameters at 10%, 50%, and 90% cumulative volume, respectively. All results were the average of three replications.

Optical microscopy: The structure of the emulsions observed using an optical microscope (Olympus BX41, Japan). A droplet of the no-diluted emulsion was placed on a microscope slide, covered with a coverslip then visualized at a magnification of 400. An image of the sample was acquired using digital image software and stored on a personal computer.

Determination of emulsifying properties: The emulsifying properties of emulsions were measured according to the method of Li, Huang, Peng, Shan, and Xue (2014). 50 mL of emulsions were immediately sampled and diluted 100 times using 0.1% sodium dodecyl sulfate (SDS). The absorbance of the emulsion at 500 nm was recorded immediately (A_0) and after 10 min (A_{10}) using a spectrophotometer (Rayleigh, 2601-UV/VIS, China). The emulsifying activity index (EAI) and emulsion stability index (ESI) were computed using Eqs. (5) and (6), respectively.

$$EAI\left(\frac{m^2}{g}\right) = 2 \times T \times \frac{A_0 \times N}{1000 \times \theta \times L \times C} \tag{5}$$

$$ESI\,(min) = \frac{A_0}{A_0 - A_{10}} \times (T_{10} - T_0) \tag{6}$$

where T equals to 2.303; A_0 is the absorbance at 0 min; N is the dilution factor (100); Θ is the proportion of the oil phase; L is the thickness of the cuvette (1 cm); C is the concentration of SPI (g/mL); A_{10} is the absorbance at 10 min; T_0 represents 0 min; and T_{10} represents 10 min.

Determination of Free Protein Concentrations. After 24 h of

storage, emulsions were transferred to centrifuge at 1000 g for 20 min. The serum phases were collected and then used for further analysis of the free protein concentrations. The free protein concentration in the serum phase was determined by a modified Lowry method. The reaction solution [a mixture of solution A (0.5%$CuSO_4$. $5H_2O$ and1% $Na_3C_6H_5O_7$. $2H_2O$) and solution B (2%Na_2CO_3 and 0.4%NaOH)] was added to the serum phase (0.5 mL) of each sample, followed by the addition of the Folin-Ciocalteu reagent. The absorbance of the solutions was measured at 650 nm by a UV/visible spectrophotometer (Rayleigh, 2601-UV/VIS, China). A calibration curve was produced using bovine serum albumin as the standard (Cho, Decker, & McClements, 2010).

Determination of surface hydrophobicity (H_0): Surface hydrophobicity was measured using the 1-anilino-8-naphthalene sulfonate (ANS) as the fluorescence probe. An aliquot of ANS solution (20 μL, 8.0 mM phosphate buffer) was added to 4 mL of sample. Fluorescence intensity (FI) was measured with a fluorescence spectrometer (Hitachi, Ltd., Tokyo, Japan) at wavelengths of 390 nm (excitation) and 470 nm (emission). The initial slope of the FI versus protein concentration plot (calculated by linear regression analysis) was used as an index of protein hydrophobicity.

2.2.5. Microencapsulation

5% w/v of maltodextrin was added to emulsion samples and microcapsules were prepared by spray drying of the prepared emulsions on a laboratory-scale mini spray dryer (two-flow nozzle, counter-current; Soroush, Iran). The operational conditions of spray drying were: air inlet temperature of 200 °C, air outlet temperature of 80 °C, and nozzle air pressure of 310 kPa. The microencapsulation powder was collected and stored in opaque air tight containers at 4 °C for further tests.

2.2.6. Physicochemical characterization of microcapsules

Encapsulation efficiency: The method described in Soottitantawat et al. (2005) to calculate encapsulation efficiency was adapted: The amount of limonene in the powder was measured as follows. 1 g of the spray dried powder was dispersed in 20 mL of water in a glass bottle, and 20 mL hexane was added, followed by forceful mixing with a vortex mixer for 1min. To extract encapsulated limonene into the organic solvent, the mixture was heated in a heating block at 45 °C for 20 min with intermittent shaking. Then, after cooling down, centrifuged at a 4000 rpm for 20 min finally the amount of limonene in the sample was measured by a UV/visible spectrophotometer (Rayleigh, 2601-UV/VIS, China) at a wavelength of 252 nm. The total amount of limonene release (LR) and the total amount of initial loaded limonene in SPI fibril microcapsule (LL) were used in the following equation to estimate limonene encapsulation efficiency (EE) Eq. (7):

$$E = \frac{LR}{LL} \times 100 \tag{7}$$

Particle size of microcapsules: Laser diffraction particle sizer (SALD-2101, Shimadzu, Japan) measured particle size distribution of the microcapsules. The dispersion powder prepared in ethanol and particle size based on equations (1) and (2) were calculated.

Scanning electron microscopy (SEM): The morphology of the microcapsules obtained from spray drying was observed using a scanning electron microscope (Leo 1450VP SEM). The samples were attached to aluminum stubs using double-sided adhesive tape and vacuum coated with gold. SEM photographs were taken at the required magnification at room temperature and examined an acceleration voltage of 20 Kv.

Fourier transforms infrared spectroscopy (FTIR): The FTIR measurements were done on microcapsules. About 1 mg of sample powder was mixed with the potassium bromide (KBr) and pressed into pellet. FTIR spectra samples were obtained using a FTIR spectrophotometer (Shimadzu 6650, Japan), at 4 cm^{-1} resolution in frequency range between 400 and 4000 cm^{-1}.

2.2.7. Optimization with VIKOR

The multi-criteria measure for compromise ranking is developed from the *Lp*-metric used as an aggregating function in a compromise programming method (Opricovic & Tzeng, 2007);

$$L_{p,j} = \left\{ \sum_{i=1}^{n} \left[\frac{w_i (f_i^* - f_{ij})}{(f_i^* - f_i^-)} \right]^p \right\}^{\frac{1}{p}}$$

where $L_{1,\,j}$ and $L_{\infty,\,j}$ are used to formulate ranking measure; $f_{i\,j}$ is the value of the i_{th} criterion function for the alternative A_j; and n is the number of criteria. The compromise ranking algorithm VIKOR is implemented carrying the following steps (Opricovic & Tzeng, 2004):

Step 1. Determine the best and the worst values of all criterion functions.

The best (f_i^*) and the worst (f_i^-)) values of all criterion functions are determined, taking into account that, if the i_{th} function represents a benefit then:

$$\begin{cases} f_i^* = max_j f_{ij} \\ f_i^- = min_j f_{ij} \end{cases} \tag{8}$$

While if the i_{th} function represents a cost then:

$$\begin{cases} f_i^* = max_j f_{ij} \\ f_i^- = min_j f_{ij} \end{cases} \tag{9}$$

Step 2. Compute the values S_j and R_j

The values S_j and R_j are calculated by the relations:

$$S_j = \sum_{i=1}^{n} \frac{w_i (f_i^* - f_{ij})}{f_i^* - f_i^-} \tag{10}$$

and

$$R_j = max_i \frac{w_i (f_i^* - f_{ij})}{f_i^* - f_i^-} \tag{11}$$

where w_i is the weight of criteria, it expresses the decision-maker's preference as the relative importance of the criteria.

Step 3. Compute the values Q_j

The values Q_j are calculated by the relation

$$Q_j = v \frac{S_j - S^*}{S^- - S^*} + (1 - v) \frac{R_j - R^*}{R^- - R^*} \tag{12}$$

where $S^* = min_j\, S_j$; $S^- = max_j\, S_j$; $R^* = min_j\, R_j$; $R^- = max_j\, R_j$ and v is introduced as a weight for the strategy of maximum group utility, while (1 − v)is the weight of the individual regret. The solution obtained by $min_j\, S_j$ is with a maximum group utility ('majority' rule), and the solution obtained by $min_j\, R_j$ is with a minimum individual regret of the 'opponent'.

Step 4. Rank the alternatives.

Rank the alternatives, sorting by the values *S*, *R* and *Q* in decreasing order. The results are three ranking lists.

2.2.8. Statistical analysis

All measurements were carried out at least in triplicate, and the data were statistically processed by analysis of variance (ANOVA) and Duncan's post-hoc test using the SPSS 21.0 statistical software package.

3. Results and discussion

3.1. Formation and structure of fibrils

Formation of SPI fibrils was monitored by ThT fluorescence assay during 24 h of incubation at 85 °C. As shown in Fig. 1, Different stages were observed during the formation of fibrils. First, there was a lag phase during which no fibrils were formed. After a certain lag time (30 min), nucleation started and the intensity of ThT was increased for

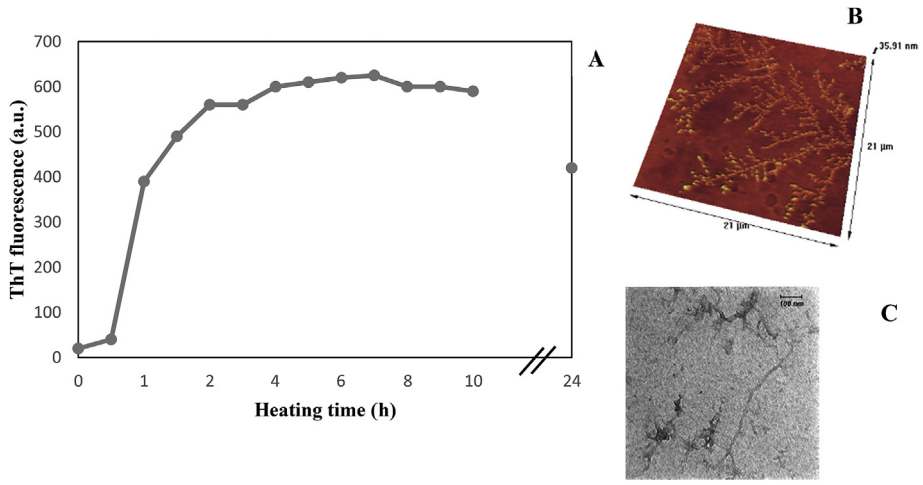

Fig. 1. Thioflavin T fluorescence intensity during incubation of SPI solution pH 2, at 85 °C (A). AFM (B) and TEM (C) images of SPI fibrils at pH 2.

2 h (growth phase). Afterwards, the growth rate remained constant (from 2 h to 8 h). Eventually, the growth rate decreased, indicating either a limitation in monomer supply or a thermodynamic equilibrium (Nielsen et al., 2001). Mudgan et al. (2009) reported that heating for more than 10 h may cause hydrolysis of beta-lactoglobulin fibrils, as a result ThT fluorescence intensity decreased. The TEM and AFM images of SPI fibrils showed that their thickness varied from 1 to 10 nm and their structure were highly branched (Fig. 1). Akkermans et al. (2008) reported the fibrils of soy glycine are 1 µm in length and a few nanometers in thickness and have abundant strand like structures.

3.2. Characterization of emulsion prepared with native and SPI fibril

3.2.1. Surface and interfacial tensions

Surface and interfacial tensions are considered as the most effective factors on the formation and stabilization of emulsions. The results concerning the effect of SPI fibrils on the surface tension of the aqueous phase are shown in Table 1. The addition of SPI fibrils to the emulsion (O/W) system led to a significant decrease ($P < 0.05$) in the surface tension of the aqueous phase compared with that of pure water (71.99 ± 0.05 mN/m). Moreover, after the addition of SPI fibrils, the interfacial tension of the emulsions showed a significant decrease from 28.35 ± 0.04 to 5.11 ± 0.05 mN/m (at concentration 0.5% w/v SPI fibril) at 25 °C (Table 1). This could be associated to the amphiphilic nature of proteins, whose ability could be located in the interface of water/oil and the formation of a stable elastic membrane (Cho et al., 2010). The interfacial tension of the native SPI solutions (10.99 ± 0.06 mN/m) was very different from that of SPI fibril solutions (5.11 ± 0.04 mN/m) at the same concentration of 1% (w/v). The lower values of interfacial tension in the emulsions prepared with SPI fibrils can induce more stability in these double-phase systems. These results properly conformed the findings of other researchers. Serfert et al. (2014) observed a considerable difference between the interfacial tensions of the sunflower oil in water emulsions prepared with native WPI (11–12 mN/m), and WPI fibrils (8–10 mN/m). Isa et al. (2011) who studied β-lactoglobulin fibrils and N.-P. K. Humblet-Hua, van der Linden, and Sagis (2013) who performed a research on lysozyme and ovalbumin fibrils, observed dramatic declines in the interfacial tension of oil in water emulsions, which could result in the stabilization of emulsions. As observed in Table 1, with an increase in the concentration of SPI fibril up to 1% (w/v), interfacial tension decreased significantly ($P < 0.05$). However, at higher concentrations, not only the decrease was not considerable, but also this parameter increased slightly (Table 1), which was caused by the higher concentration of protein rather than by critical micelle concentration (CMC) (Dickinson, 2012). At concentrations higher than 1% (w/v), it seems that after saturating the interface and being monodispersed in the aqueous phase, the excess protein molecules were aggregated and formed a micelle in the aqueous phase due to their amphiphilic character through hydrophobic interactions. As a result, after CMC, the increase in the protein concentration had no effect on the interfacial tension (Dickinson, 2012).

Table 1
The surface and interfacial tensions of the emulsions prepared with native SPI and different concentrations of SPI fibril at 25 °C.

sample	Surface tension (mN/m)	interfacial tension (mN/m)
Water	71.99 ± 0.05^{a}	28.35 ± 0.04^{a}
Native SPI (1%)	42.29 ± 0.03^{c}	10.99 ± 0.06^{b}
Different concentration fibril SPI		
0.1%	46.03 ± 0.07^{b}	13.99 ± 0.02^{b}
0.3%	44.12 ± 0.13^{b}	10.65 ± 0.11^{b}
0.5%	41.43 ± 0.03^{c}	5.04 ± 0.05^{d}
1%	41.67 ± 0.02^{c}	5.11 ± 0.04^{d}
1.5%	41.99 ± 0.02^{c}	8.34 ± 0.08^{c}
2%	42.89 ± 0.08^{c}	9.99 ± 0.07^{c}

Values are mean ± SD (n = 3). Means in the Superscript (horisontal) followed by different letters are significantly different ($p < 0.05$).

3.2.2. Zeta potential

The results in Table 2 revealed that all of the droplet surfaces were positively charged in all of the SPI emulsions, which was expected considering the isoelectric point of SPI (pH = 4.6) and the pH of the samples (pH = 3.5). Moreover, the increase in the SPI fibrils concentration up to 1% (w/v) elevated the zeta potential of the samples. However, exceeding this value did not have a remarkable effect on the zeta potential of the samples. This reveals that the SPI fibrils concentration of 1% is appropriately capable of covering the oil-water interface (Table 2). It can be declared that with an increase in the protein concentration, the intermolecular spaces decrease, and consequently the particles can join together and form a larger aggregation. In this case, not only the number of charged groups is reduced, but also the distribution of the charged chains on the particle surfaces causes a change in the zeta potential of the new structure. Hu, McClements, and Decker (2003) reported that the rise in the concentration of β-lactoglobulin fibrils up to 2% (w/v) significantly increased the zeta potential of the corn oil/water emulsion droplets. At higher concentrations, the emulsion droplet surfaces were saturated with the protein and the zeta potential no longer changed remarkably. In addition, it can be seen in Table 2 that the zeta potential of the native SPI solutions (+25.12 ± 2.68 mV) and the SPI fibrils (+34.91 ± 5.04 mV) were

Table 2
The physicochemical properties of the emulsions prepared with the native SPI and different concentrations of SPI fibril.

Emulsion (wall materials)	Concentration (%)	Zeta potential mV	Emulsion droplet size D_{43}(μm)	specific surface (m^2/ml)	span
Native SPI	1	+25.12 ± 2.68^{c}	6.63 ± 0.81^{c}	2.47 ± 0.53^{b}	1.37 ± 0.14^{d}
Fibril SPI (mg/ml)	0.1	+23.08 ± 3.42^{d}	10.87 ± 0.72^{a}	1.37 ± 0.42^{c}	1.98 ± 0.43^{a}
	0.3	+26.91 ± 5.04^{c}	4.34 ± 1.72^{b}	1.97 ± 0.27^{c}	1.77 ± 0.27^{b}
	0.5	+33.67 ± 3.64^{a}	1.54 ± 0.35^{c}	3.53 ± 0.32^{a}	1.16 ± 0.12^{e}
	1	+34.91 ± 5.04^{a}	2.65 ± 0.58^{b}	3.13 ± 0.14^{ab}	1.25 ± 0.22^{e}
	1.5	+34.61 ± 5.04^{a}	2.51 ± 0.84^{b}	2.67 ± 0.21^{b}	1.34 ± 0.34^{d}
	2	+31.03 ± 2.48^{b}	3.09 ± 1.14^{b}	1.87 ± 0.78^{c}	1.64 ± 0.28^{c}

Values are mean ± SD (n = 3). Means in the Superscript (horisontal) followed by different letters are significantly different ($p < 0.05$).

significantly ($p < 0.05$) different from each other at the same concentration. It could be justified that the SPI fibrils were partially unfolded during formation by heating at pH = 2 and the charged groups which had been hidden in the molecule, were moved to the surface and apparently led to a more positive zeta potential.

3.2.3. Emulsion droplet size

The variations in the emulsion droplet sizes in response to the different levels of the SPI fibrils concentration showed that as the protein concentration increased up to 1% (w/v), the droplet diameters decreased. However, as the concentration increased from 1 to 2%(w/v), the droplet sizes increased (Table 2) Gao et al. (2017) reported that as the concentration of β-lactoglobulin fibril increased up to 5 mg/mL, the O/W emulsion droplets size were small and uniform, indicating that the fibrils covered the droplets efficiently. Nevertheless, by increasing the concentration up to 25 mg/mL, a sudden increase was observed in the droplet sizes which caused a reduction in the steric repulsion forces between the droplets due to their low surface zeta potential. Therefore, the droplets coalesced and formed larger ones. The largest droplets in the emulsion prepared with 0.1% (w/v) SPI fibrils, had an average size of 10.87 ± 0.72 μm. It can be justified that at low concentrations, protein cannot cover the droplet surfaces completely and the steric and electrostatic repulsion between the droplets are weak which cannot prevent them from flocculating (Dickinson, 2012). By comparing the emulsion droplet sizes in the solutions of native SPI and SPI fibril at the same concentration of 1% (w/v), the average droplet sizes were 6.63 ± 3.64 μm and 2.65 ± 3.64 μm respectively. The protein fibrils caused the interfacial tension to decrease, and hence it was expected that the emulsion droplet size would get smaller. Specific surface is one of the determining factors of emulsion stability. The higher this factor, the more stable the emulsion. As indicated in Table 2, the emulsion prepared with 0.5% (w/v) SPI fibrils had the highest specific surface. It should be noted that at this concentration, the lowest span (1.16 ± 0.12) was observed (Table 2). Serfert et al. (2014) stated that the oil droplets of the emulsion stabilized with the fibrils of whey protein and β-lactoglobulin had a more uniform distribution and a smaller span respectively, compared with those of the emulsions stabilized with the native form of the above-mentioned proteins.

3.2.4. Emulsifying properties

Emulsifying property indicates the ability of a protein to adsorb to the oil/water interface, and to bring about emulsion stability which is evaluated using the emulsifying activity index (EAI) and emulsifying stability index (ESI) (Zhao, Dong, Li, Kong, & Liu, 2015). The assessment results of the emulsifying properties are depicted in Fig. 2. The EAI (38.02 m^2/g) and ESI (23.5 min) of the emulsion prepared with 1% (w/v) SPI fibril were significantly higher than those (31.21 m^2/g and 15 min) of the sample prepared with the native SPI. This could be due its high rigidity and thus low flexibility at the o/w-interface in acidic pH at native SPI (Serfert et al., 2014). Because, when preparing the fibril, SPI molecules unfold partially and the hydrophobic groups which are normally hidden in the molecule, are more exposed to the surrounding environment. Thus, the emulsifying property of the fibril was significantly ($P < 0.05$) higher than that of the native SPI, leading to the emulsion stability and a decrease in the phase separation rate (McClements, 2005). These findings are consistent with those of Zhao et al. (2015) who did research on the emulsifying property of the heated and unheated SPI. Blijdenstein, Veerman, and van der Linden (2004) cited that the presence of β-lactoglobulin fibril in emulsions reduced the emulsion creaming and enhanced the emulsion stability dramatically. They also stated that the β-lactoglobulin fibril remarkably decreased the emulsion flocculation and stabilized the emulsion at a minimum concentration of the fibril.

3.2.5. Free protein contents

The SPI fibril concentration was elevated from 0.1 to 1% (w/v), the free protein content decreased considerably; however, it increased when the SPI fibril concentration increased from 1 to 2% (w/v) (Fig. 3). As mentioned earlier, it can be said that there was not enough protein to cover the limonene droplets completely at the concentrations lower than 0.5%(w/v); consequently, the limonene droplets coalesced and the protein was freely present in the continuous phase. At the concentrations higher than 0.5%(w/v), the adsorption behavior of protein at the water-oil interface was in a way that the emulsion droplet surfaces are saturated with protein and are even located as a multilayer and the remainder is freely present in the system. These results are in agreement with the previous ones based on which the rise in the heated protein concentration led to the stability of the emulsion with smaller droplets (Cho et al., 2010). Gao et al. (2017) also reported that as β-lactoglobulin fibril concentration increased; the loaded surfaces of the emulsion particles partly increased and remained constant thereafter. As illustrated in Fig. 3, the free protein contents in the SPI fibril sample were lower than the native SPI at the same concentration. In the SPI fibril, the molecule is more flexible and a larger number of hydrophobic groups will come to the surface of the particle, causing the hydrophobicity to increase and the interfacial tension to decrease. Therefore, more protein will be stabilized on the particle surface (McClements, 2005). Previous studies have also suggested that the thermal treatment of soy protein brought about a significant increase in its hydrophobicity compared with the unheated sample (Tezuka, Yagasaki, & Ono, 2004).

3.2.6. Surface hydrophobicity (H_0)

The H_0 values of native SPI and SPI fibril concentration were shown in Fig. 4. The H_0 value of SPI fibril (1% w/v) was higher than native SPI in the same concentration of 1% (w/v). During the formation of fibrils, protein molecules are structurally rearranged and these denatured proteins had tendency to expose their hydrophobic zones to the aqueous medium, which resulted in higher H_0 value in SPI fibril. This phenomenon not only decreases the surface tension, but also create a physical barrier to reduce the possibility of particle aggregation and/or oil droplets flocculation (Jordens et al., 2014). Keerati-u-rai and Corredig (2009) reported that heating the soy protein before

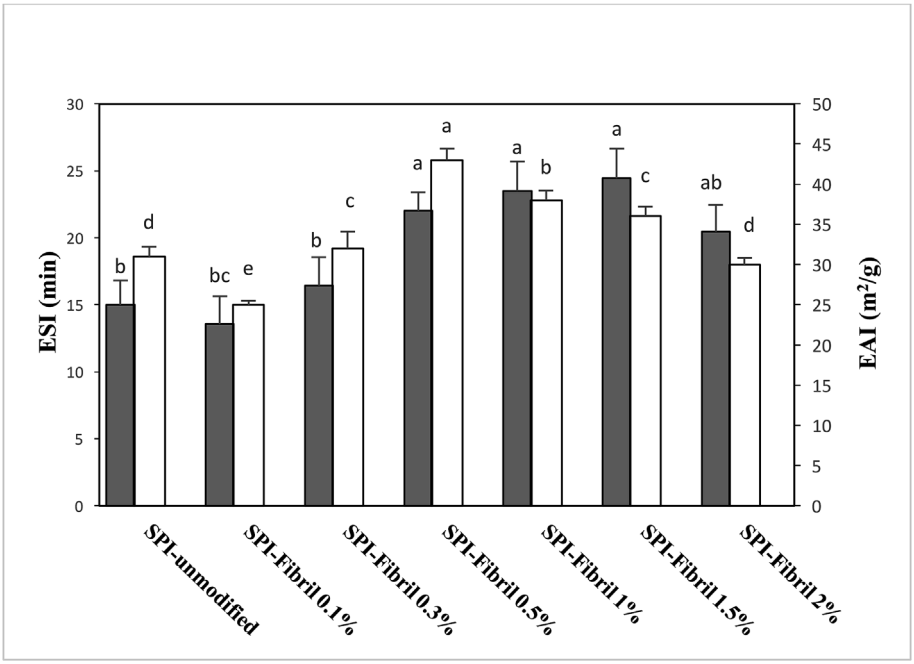

Fig. 2. ESI and EAI of the emulsions prepared with the native SPI and the different concentrations of SPI fibril. The filled bar represent the ESI and the no-filled (blank) bar represent the EAI.

emulsification resulted in the loading of more protein at the oil-water interface. In addition to hydrophobicity, the amount of the electric charge and the flexibility of the molecule play important roles in the adsorption of protein at the oil-water interface. As shown in Fig. 4, by increasing the concentration of fibril to 1% (w/v) the H_0 values raised from 354 to 875 and then declined to 593.

3.3. Characterization of microcapsules prepared with native and SPI fibril

3.3.1. The particle size and encapsulation efficiency of the microcapsules

The results indicated that the rise in the protein concentration had a significant effect on the size of the microcapsules obtained from spray drying (Table 3). Among the samples, the microcapsules resulting from the emulsion comprising 0.5% (w/v) SPI fibril had larger size. At the same time, the corresponding emulsion had the smallest droplet size. The increase in the powder particle size could be attributed to the emulsion droplet sizes among which the smaller ones were covered with a thicker layer of the wall material during drying (Mohammadzadeh, Koocheki, Kadkhodaee, & Razavi, 2013). It should also be noted that with the rise in the powder particle size, the limonene content in the microcapsules increased, too (encapsulation efficiency, Table 3) which could be ascribed to the thickening of the microcapsule walls. Emulsion droplet size and wall material concentration are the two major factors in determining encapsulation efficiency (Jafari, Assadpoor, He, & Bhandari, 2008). With a rise in the fibril concentration up to 1% (w/v), the encapsulation efficiency improved remarkably

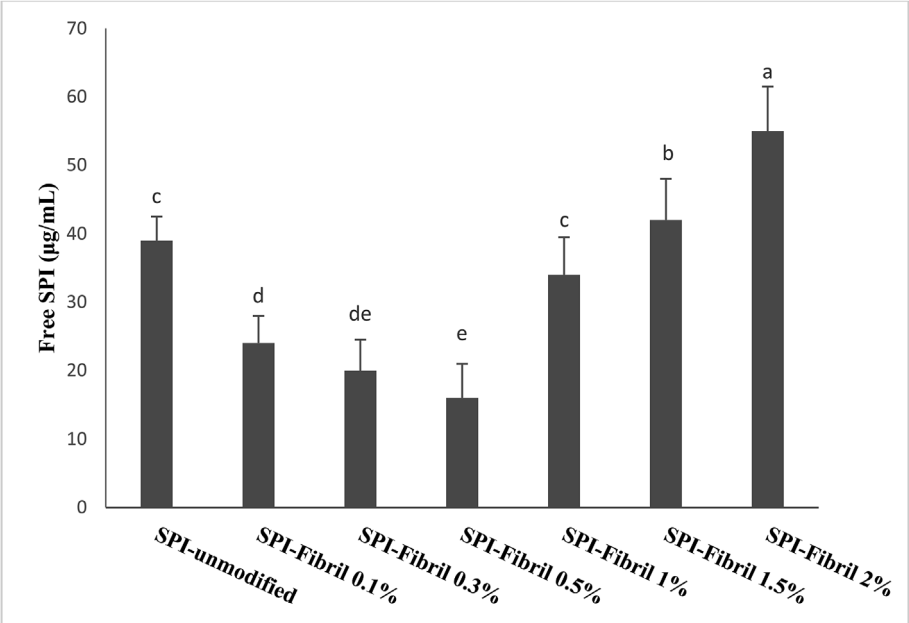

Fig. 3. The free protein contents of the emulsions prepared with the native SPI and the different concentrations of SPI fibril.

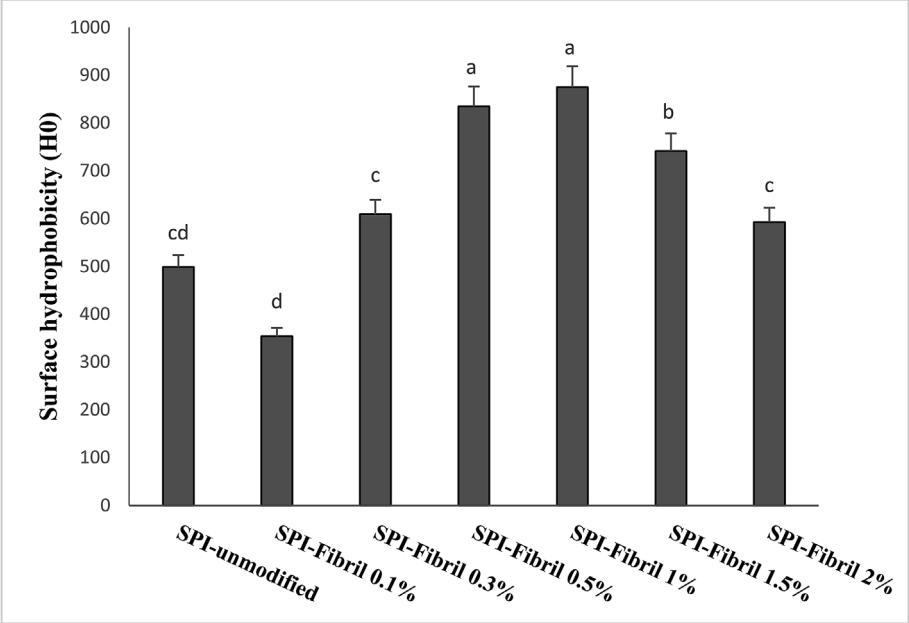

Fig. 4. The surface hydrophobicity (H_0) of the emulsions prepared with the native SPI and the different concentrations of SPI fibril.

and showed a negligible decrease thereafter. The highest encapsulation efficiency (65.47 ± 4.23%) belonged to the microcapsules prepared with 0.5% (w/v) fibril. As observed earlier, the heterogeneity of the particle size distribution was reduced in the presence of the SPI fibril rather than the native SPI at the same concentration of 1% (w/v). This characteristic significantly affected the resistance of the droplets against the shear stress of the atomizer. Moreover, it influenced the wall formation rate and the retention of the core material during drying (Noshad, Mohebbi, Shahidi, & Koocheki, 2015). Therefore, the encapsulation efficiency was equal to 58.47 ± 4.87% for the microcapsules obtained from the SPI fibril and 49.19 ± 4.62% for the ones resulting from the native SPI. Similar findings have also been presented by Serfert et al. (2014) about the enhancement of the encapsulation efficiency by fibrils in comparison with their source proteins. In that research, the encapsulation efficiency was equal to 88.5% for the microcapsules obtained from the native whey protein and 95–95.6% for the samples produced from its fibril (Serfert et al., 2014).

3.3.2. Light microscopy and scanning electron microscopy (SEM)

Comparing the light microscopy images of the different emulsions after 12 h showed that the emulsion prepared with 0.1% (w/v) SPI fibril had larger droplets and a broader particle size distribution than the other emulsions did (the coalescence of the emulsion droplets was observed) (Fig. 5). As the fibril concentration increased, the homogeneity of the particles increased, whereas they became smaller. These images are in a proper agreement with the results obtained from the particle sizer apparatus. As the emulsion stability increases and the droplet sizes decrease during drying, a more adequate network and a more homogenous coverage of wall material is formed around them. This has a positive effect on the limonene content of the encapsulated and on preventing it from diffusing out (Noshad et al., 2015). Given the SEM images (Fig. 5), it was observed that with a rise in the fibril concentration, the fracture and dent of the microcapsule structures in addition to the fractures of their walls decreased. Furthermore, comparison between the microcapsules obtained from the emulsions containing 1% (w/v) SPI fibril and the native SPI confirmed the two following points: 1- the microcapsules obtained from the SPI fibril were smaller and more homogenous. 2- Their surfaces were smoother. These findings conformed to those of Serfert et al. (2014) who compared the SEM images of the microcapsules resulting from β-lactoglobulin fibril and the native β-lactoglobulin.

3.3.3. Fourier transform infrared (FTIR) spectroscopy

FTIR was performed to determine the structure of the microcapsules. The infrared spectra of the raw material and the microcapsules prepared with the native SPI or various concentrations of the SPI fibril and the limonene core were in the range of 500–4000 cm^{-1} at room temperature (25 °C) (Fig. 6). In the limonene spectrum, some peaks were observed in the regions of 3082 cm^{-1} (=C-H), 2835-2965 cm^{-1} (aliphatic C-H), 1644 cm^{-1} (C=C), 1437 cm^{-1} (CH_2 bending) and 1375 cm^{-1} (CH_3 bending) (Partal Ureña, Moreno, & López González, 2009). The peaks observed in both the spectra of the native SPI and the SPI fibril were as follows: 3000-3500 cm^{-1} (O-H stretching and N-H stretching), 3060 cm^{-1} (aromatic C-H), 2933 cm^{-1}

Table 3
The physicochemical properties of the microcapsules obtained from the native SPI and different concentrations of SPI fibril through spray drying.

Microcapsule (wall materials)	Concentration (%)	Moisture content (%)	Particle size (μm)	Encapsulation efficiency (%)
Native SPI	1	3.22 ± 0.21^{b}	7.63 ± 1.61^{b}	49.19 ± 4.62^{c}
Fibril SPI (mg/ml)	0.1	4.19 ± 0.06^{a}	5.87 ± 0.34^{d}	18.39 ± 3.28^{e}
	0.3	4.08 ± 0.16^{a}	6.34 ± 0.82^{c}	31.54 ± 5.18^{d}
	0.5	2.21 ± 0.07^{c}	8.65 ± 0.36^{a}	65.47 ± 4.23^{a}
	1	2.18 ± 0.04^{c}	8.34 ± 0.74^{a}	58.47 ± 4.87^{b}
	1.5	2.14 ± 0.11^{cd}	7.51 ± 0.21^{b}	53.98 ± 5.23^{bc}
	2	2.11 ± 0.09^{d}	7.09 ± 0.31^{b}	48.89 ± 2.19^{c}

Values are mean ± SD (n = 3). Means in the Superscript (horisontal) followed by different letters are significantly different ($p < 0.05$).

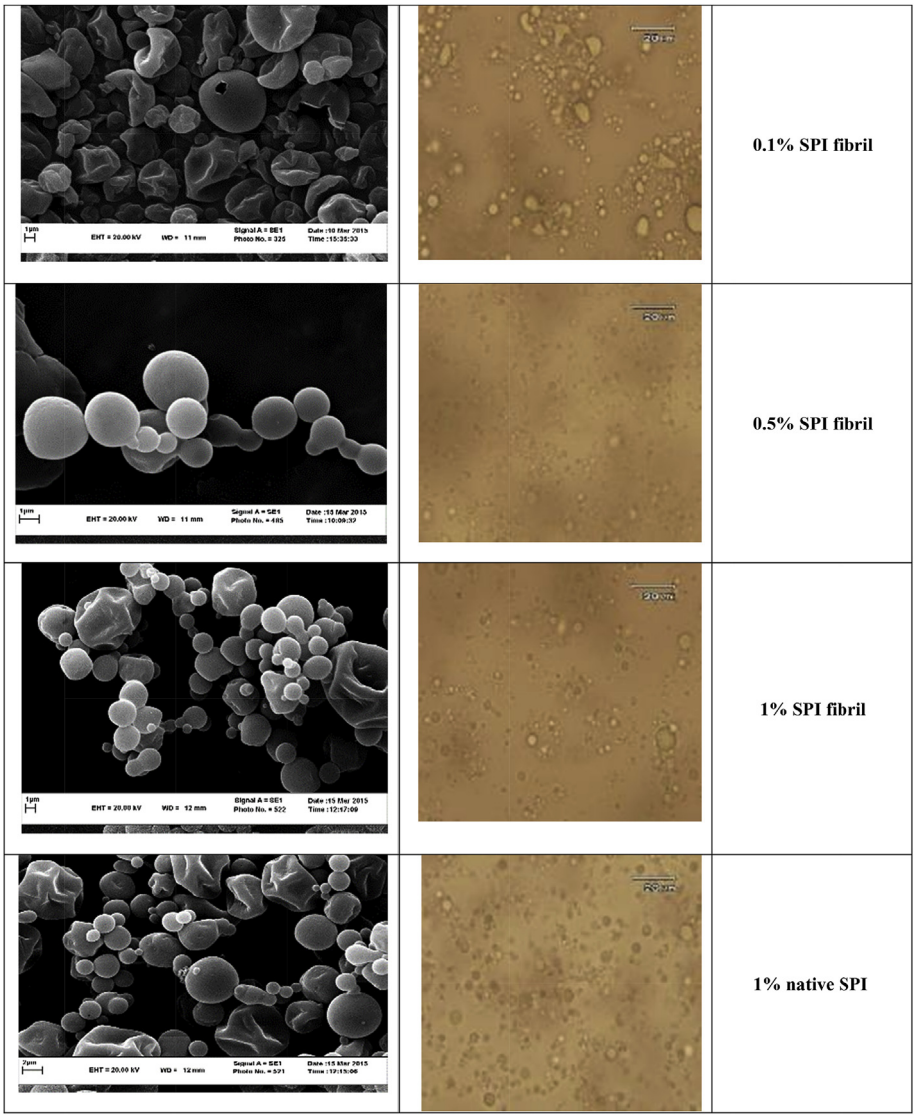

Fig. 5. The light microscopy images of the emulsions after 12 h and the SEM images of the microcapsules obtained from the native SPI and the different concentrations of SPI fibril.

(aliphatic C-H), 1662 cm^{-1} (C=O stretching), 1536 cm^{-1} (N-H bending), 1074 cm^{-1} (C-O stretching). The SPI spectrum had two bands, namely amide I (1646 cm^{-1}) and amide II (1540 cm^{-1}), which are two of the typical FTIR spectra of proteins (Zhang, Yang, Zhao, Hua, & Zhang, 2014). Based on the FTIR spectrum, the structural differences between the SPI fibril and the native SPI include changes in wavenumber and area under peak at 3287, 1662 and 1723 cm^{-1} which are associated with β-sheets and the formation of hydrogen bonds between the amine and carbonyl amide functional groups and formation of two new peaks at 2550 cm^{-1}which is related to the free –SH groups. These hydrogen bonds are stronger and wider in the β-sheets of the fibrils than in the α-helix of the native SPI, due to the shorter distance between these two functional groups (Zhang et al., 2014). As mentioned earlier, SPI structure was partially unfolded during the fibril formation and the rearrangement of the oligomers was in a way that α-helix changed into β-sheets and more sulfhydryl and hydrophobic groups were located on the surface (Keerati-u-rai & Corredig, 2009; Tezuka et al., 2004). That is why the performance of the SPI fibril was better in forming and stabilizing the emulsion than that of the native SPI at the same concentration of 1% (w/v). This fact was featured in the FTIR spectra of the two samples via the difference in the intensity and resolution of the peaks. Tezuka et al. (2004) claimed that the thermal treatment of SPI caused an increase in the absorbance intensity of the I and II amides bands. It also brought about the displacement of amide I towards higher wavelengths (1646-1654 cm^{-1}), showing the structural changes in SPI. The FTIR spectra of different concentrations of the SPI fibril are exhibited in Fig. 6. The peaks (3421, 2931, 1435) corresponding to the functional groups of –NH and –CH can be clearly observed in the spectrum of the 0.5% (w/v) sample as compared with that of the 0.1% (w/v) one. This indicates that 0.5% (w/v) SPI fibril could better cover the limonene particles than 0.1% (w/v). Nevertheless, as the concentrations was elevated from 1 to 2% (w/v), the resolution of the peaks decreased again. This confirms that the fibril was removed from the limonene particles when its concentration was increased. The content of the protein adsorbed at the surface of the emulsion droplets also confirms these findings. The peaks at 1368 cm^{-1} (CH_3) and 1416 cm^{-1} (CH_2 bending) in the spectra of the microcapsules were associated with limonene, confirming the presence of limonene in the microcapsules. No spectrum depicted limonene structural change or its combination with the SPI fibril. It should be pointed out the peaks at 1027, 1080 and 1153 cm^{-1} pertained to the etheric bond because of the presence of maltodextrin in the microcapsules system.

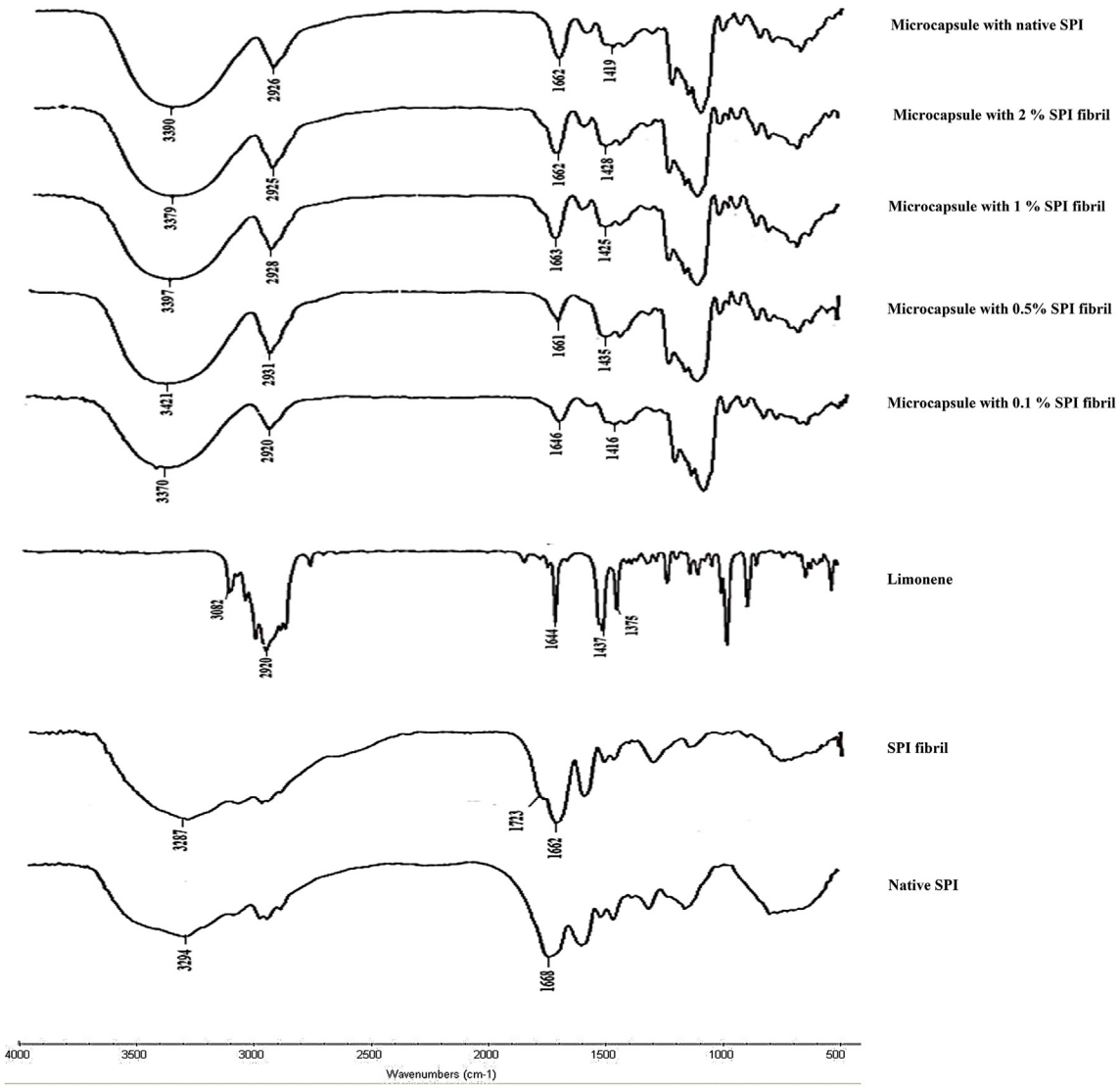

Fig. 6. The infrared spectra of the raw material and the microcapsules prepared with the native SPI and various concentrations of the SPI fibril and the limonene core were in the range of 500–4000 cm^{-1}.

3.4. Selection of the best concentration SPI fibril through the VIKOR method

The VIKOR method was developed for multi criteria optimization of complex systems. It determines the ranking-list, the compromise solution, and the weight stability intervals for preference stability of the compromise solution obtained with the initial (given) weights. This method focuses on ranking and selecting from a set of alternatives in the presence of conflicting criteria. It introduces the multi criteria ranking index based on the particular measure of "closeness" to the "ideal" solution (Opricovic & Tzeng, 2007). In this study, we determined the effect of different SPI fibril concentrations on properties of emulsion and microencapsulated limonene. However, decision making for ideal SPI fibrils concentration for microencapsulation was very difficult because there were fifteen different results influencing the emulsion and microcapsule characteristic (surface and interfacial tension, zeta potential, emulsion droplet size, specific surface, span, EAI, ESI, free protein, Surface hydrophobicity, optical microscopy, SEM, particle size of microcapsule, encapsulation efficiency, FTIR). These factors had different units and some of them were in the form of spectrum or image, therefore, we used the VIKOR approach for ease of comparison. The first step was to develop the decision making matrix. In this matrix, columns denote the scales (measured attributes) and rows show the choices (various concentrations of the SPI fibril) which should be compared with each other. Subsequently, the weights of the indices were obtained through the entropy method (Table 4). After that, the ideal positive and negative values were calculated using Equations (8)–(10) which are presented in Table 5. S_i, R_i and Q_i were calculated for each choice (Table 5). As can be seen the Q_i values, were 0.5073, 1.000, 0.9020, 0.0045, 0.0435, 0.0599 and 0.1210 for respectively native SPI, 0.1, 0.3, 0.5, 1, 1.5 and 2% (w/v) SPI fibril. The final rankings of SPI fibril concentration were performed according to Q_i and the lowest Q_i ranked first. In the present study, given the 15 considered performance evaluation scales, 0.5% (w/v) SPI fibril was chosen as the best.

4. Conclusion

In this study emulsifying and microencapsulation properties of SPI fibrils were compared to native SPI for the first time. The results clearly showed the potential of SPI fibrils as a functional ingredient with respect to emulsifying and microencapsulation properties and stability of (spray dried) limonene emulsions in comparison to native SPI. VIKOR method showed that 0.5% (w/v) fibril concentration was sufficient to provide the best emulsifying property and suitable microencapsulation

Table 4
The weights of the decision indices through the entropy method and ideal positive and negative values.

	Surface tension (Mn/m)	Interfacial tension (Mn/m)	Zeta potential (mV)	Emulsion droplet size (μm)	Specific surface (ml/m^2)	span	EAI (min)	ESI (m2/g)	free protein (μg/mL)	Optical microscopy	SEM	Surface hydrophobicity	Microcapsule particle size (μm)	Encapsulation efficiency (%)	FTIR
Ej	0.9996	0.9708	0.9953	0.9468	0.9795	0.9913	0.9887	0.9931	0.9608	0.9550	0.9655	0.5414	0.9958	0.9012	0.9552
Dj	0.0003	0.0291	0.0046	0.0531	0.0204	0.0086	0.0112	0.0068	0.0391	0.0449	0.0483	0.4585	0.0041	0.0987	0.0447
wj	0.0003	0.0326	0.0052	0.0596	0.0229	0.0097	0.0126	0.0076	0.0439	0.0504	0.0513	0.5148	0.0046	0.1109	0.0448
F^+	41.43	5.04	34.91	1.34	3.53	1.16	24.43	43	16	5	5.34	4.19	8.65	65.47	5
F^-	46.03	13.99	23.08	6.87	1.37	1.97	13.56	25	55	1	1.62	2.11	5.87	18.39	1

Table 5
S_i, R_i and Q_i for each choice.

Microencapsulate (wall material)	Concentration (%)	S_i	R_i	Q_i	Ranking
Native SPI	1	0.4360	0.2747	0.5073	5
SPI fibril	0.1	0.8441	0.5148	1.0000	7
	0.3	0.7291	0.4876	0.9020	6
	0.5	0.0275	0.0247	0.0045	1
	1	0.0986	0.0282	0.0435	2
	1.5	0.1105	0.0292	0.0599	3
	2	0.1862	0.0439	0.1210	4

of limonene. Excessive fibrils would result in larger emulsion droplet size, although the stability was acceptable. Thus, SPI fibrils appear to be promising carriers for different delivery systems, such as nutraceutical, cosmetic or pharmaceutical products.

References

Akkermans, C., van der Goot, A. J., Venema, P., van der Linden, E., & Boom, R. M. (2008). Formation of fibrillar whey protein aggregates: Influence of heat and shear treatment, and resulting rheology. *Food Hydrocolloids, 22*(7), 1315–1325.

Blijdenstein, T. B., Veerman, C., & van der Linden, E. (2004). Depletion− flocculation in oil-in-water emulsions using fibrillar protein assemblies. *Langmuir, 20*(12), 4881–4884.

Chang, C., Niu, F., Gu, L., Li, X., Yang, H., Zhou, B., ... Yang, Y. (2016). Formation of fibrous or granular egg white protein microparticles and properties of the integrated emulsions. *Food Hydrocolloids, 61*, 477–486.

Cho, Y.-H., Decker, E. A., & McClements, D. J. (2010). Formation of protein-rich coatings around lipid droplets using the electrostatic deposition method. *Langmuir, 26*(11), 7937–7945.

Dickinson, E. (2012). Use of nanoparticles and microparticles in the formation and stabilization of food emulsions. *Trends in Food Science & Technology, 24*(1), 4–12.

Gao, Z., Zhao, J., Huang, Y., Yao, X., Zhang, K., Fang, Y., ... Yang, H. (2017). Edible Pickering emulsion stabilized by protein fibrils. Part 1: Effects of pH and fibrils concentration. *LWT-Food Science and Technology, 76*, 1–8.

Humblet-Hua, K., Scheltens, G., Van Der Linden, E., & Sagis, L. (2011). Encapsulation systems based on ovalbumin fibrils and high methoxyl pectin. *Food Hydrocolloids, 25*(4), 569–576.

Humblet-Hua, N.-P. K., van der Linden, E., & Sagis, L. M. (2013). Surface rheological properties of liquid–liquid interfaces stabilized by protein fibrillar aggregates and protein–polysaccharide complexes. *Soft Matter, 9*(7), 2154–2165.

Hu, M., McClements, D. J., & Decker, E. A. (2003). Lipid oxidation in corn oil-in-water emulsions stabilized by casein, whey protein isolate, and soy protein isolate. *Journal of Agricultural and Food Chemistry, 51*(6), 1696–1700.

Isa, L., Jung, J.-M., & Mezzenga, R. (2011). Unravelling adsorption and alignment of amyloid fibrils at interfaces by probe particle tracking. *Soft Matter, 7*(18), 8127–8134.

Jafari, S. M., Assadpoor, E., He, Y., & Bhandari, B. (2008). Encapsulation efficiency of food flavours and oils during spray drying. *Drying Technology, 26*(7), 816–835.

Jordens, S., Rühs, P. A., Sieber, C., Isa, L., Fischer, P., & Mezzenga, R. (2014). Bridging the gap between the nanostructural organization and macroscopic interfacial rheology of amyloid fibrils at liquid interfaces. *Langmuir, 30*(33), 10090–10097.

Keerati-u-rai, M., & Corredig, M. (2009). Effect of dynamic high pressure homogenization on the aggregation state of soy protein. *Journal of Agricultural and Food Chemistry, 57*(9), 3556–3562.

Li, C., Huang, X., Peng, Q., Shan, Y., & Xue, F. (2014). Physicochemical properties of peanut protein isolate–glucomannan conjugates prepared by ultrasonic treatment. *Ultrasonics Sonochemistry, 21*(5), 1722–1727.

Loveday, S. M., Wang, X. L., Rao, M. A., Anema, S. G., & Singh, H. (2012). β-Lactoglobulin nanofibrils: Effect of temperature on fibril formation kinetics, fibril morphology and the rheological properties of fibril dispersions. *Food Hydrocolloids, 27*(1), 242–249.

McClements, D. J. (2005). Theoretical analysis of factors affecting the formation and stability of multilayered colloidal dispersions. *Langmuir, 21*(21), 9777–9785.

Mohammadzadeh, H., Koocheki, A., Kadkhodaee, R., & Razavi, S. M. (2013). Physical and flow properties of d-limonene-in-water emulsions stabilized with whey protein concentrate and wild sage (Salvia macrosiphon) seed gum. *Food Research International, 53*(1), 312–318.

Noshad, M., Mohebbi, M., Shahidi, F., & Koocheki, A. (2015). Effect of layer-by-layer polyelectrolyte method on encapsulation of vanillin. *International Journal of Biological Macromolecules, 81*, 803–808.

Opricovic, S., & Tzeng, G.-H. (2004). Compromise solution by MCDM methods: A comparative analysis of VIKOR and TOPSIS. *European Journal of Operational Research, 156*(2), 445–455.

Opricovic, S., & Tzeng, G.-H. (2007). Extended VIKOR method in comparison with outranking methods. *European Journal of Operational Research, 178*(2), 514–529.

Partal Ureña, F., Moreno, J. R. A., & López González, J. J. (2009). Conformational study of (R)-(+)-limonene in the liquid phase using vibrational spectroscopy (IR, Raman, and VCD) and DFT calculations. *Tetrahedron: Asymmetry, 20*(1), 89–97. https://doi.

org/10.1016/j.tetasy.2009.01.024.
Serfert, Y., Lamprecht, C., Tan, C.-P., Keppler, J., Appel, E., Rossier-Miranda, F., ... Selhuber-Unkel, C. (2014). Characterisation and use of β-lactoglobulin fibrils for microencapsulation of lipophilic ingredients and oxidative stability thereof. *Journal of Food Engineering, 143*, 53–61.
Soottitantawat, A., Takayama, K., Okamura, K., Muranaka, D., Yoshii, H., Furuta, T., et al. ... Linko, P. (2005). Microencapsulation of l-menthol by spray drying and its release characteristics. *Innovative Food Science & Emerging Technologies, 6*(2), 163–170.
Tezuka, M., Yagasaki, K., & Ono, T. (2004). Changes in characters of soybean glycinin groups I, IIa, and IIb caused by heating. *Journal of Agricultural and Food Chemistry, 52*(6), 1693–1699.
Wen, C., Yuan, Q., Liang, H., & Vriesekoop, F. (2014). Preparation and stabilization of D-limonene Pickering emulsions by cellulose nanocrystals. *Carbohydrate Polymers, 112*, 695–700. https://doi.org/10.1016/j.carbpol.2014.06.051.
Zhang, Y., Yang, R., Zhao, W., Hua, X., & Zhang, W. (2014). Physicochemical and emulsifying properties of protein extracted from soybean meal assisted by steam flash-explosion. *Innovative Food Science & Emerging Technologies, 23*, 131–137.
Zhao, J., Dong, F., Li, Y., Kong, B., & Liu, Q. (2015). Effect of freeze–thaw cycles on the emulsion activity and structural characteristics of soy protein isolate. *Process Biochemistry, 50*(10), 1607–1613.